Supporting Information for

Phase Segregation via Etching-Induced Cation Migration in CoS_x-ZnS Nanoarchitectures for Solar Hydrogen Evolution

Zirong Shen, Junmin Huang, Junying Chen*, Yingwei Li*,

State Key Laboratory of Pulp and Paper Engineering, School of Chemistry and Chemical Engineering, South China University of Technology, Guangzhou 510640, China

E-mail: cejychen@scut.edu.cn; liyw@scut.edu.cn

EXPERIMENTAL SECTION

Chemicals

All chemicals were purchased from commercial sources and used without further treatments unless otherwise indicated.

Synthesis of H-ZIF-8 and y-ZIF-8

ZIF-8 dodecahedra were prepared first. 0.25 g of $Zn(CH_3COO)_2$ was dissolved in 5 mL of deionized (DI) water, which was added into a 5 mL aqueous solution (DI water) containing 1.12 g of 2-methylimidazole. The resulting mixture was homogenized by stirring vigorously for 1 min, followed by letting stand at room temperature for 24 h until white powders fully formed, which were collected and washed with ethanol several times, and dried at 60 ^oC for further use. Then the as-prepared ZIF-8 dodecahedra powder was dispersed in 10 mL DI water by ultrasonication for 15 min to form a colloidal ZIF-8 solution. For the chemical etching process, 640 mg xylenol orange sodium salt (XO) was dissolved in 40 mL DI water first. By adding a certain amount of HCl or NaOH, the pH of this etchant solution could be adjusted, e.g., pH = 2.2, 2.5, 3.0. The colloidal ZIF-8 solution was added into the etchant solution with varied pH values. Then, the resulting mixture was vigorously stirred for an optimized time to obtain y-ZIF-8 with different etching degrees, where y = 1 (unetched), 2 (etching by a pH 3.0 XO solution for 6h), 3 (also as H-ZIF-8, etching by a pH 2.5 XO solution for 6 h), and 4 (etching by a pH 2.2 XO solution for 3 h), corresponding to unetched, low, optimal, and high etching degrees on ZIF-8. The resulting y-ZIF-8 was collected via centrifugation, followed by washing with deionized water and ethanol repeatedly, and dried by vacuum at 60 ^oC overnight for further usage.

Synthesis of H-ZIF-8@ZIF-67

For the heteroepitaxial growth of ZIF-67 on the y-ZIF-8 particles, 10 mg of the as-formed y-ZIF-8 powder was dispersed in 10 mL methanol by ultrasonication for 15 min, followed by dissolving

a certain amount of $Co(NO_3)_2 \cdot 6H_2O$. Next, the corresponding amount of 2-methylimidazole (8 equivalent of the cobalt salt) was dissolved in another 5 mL methanol. The above two solutions were then mixed and incubated at room temperature for 3 h under stirring. The resulting purple powders were collected via centrifugation, washed with methanol for three times, and vacuum-dried at 60 ºC for 12 h to afford y-ZIF-8@ZIF-67. By adjusting the amount of $Co(NO_3)_2 \cdot 6H_2O$ (e.g., 5, 10, 15 mg), H-ZIF-8@ZIF-67-n products, where n represents the Zn/Co mole ratios in the synthesis of the layered ZIFs, could be obtained (abbreviated as H-ZIF-8@67-n, n = 2.5, 3.5, and 5, respectively).

Synthesis of photocatalysts

In a typical synthesis, 50 mg of H-ZIF-8@ZIF-67-n and 100 mg of thioacetamide (TAA) were added into a mixed solution containing 28 mL ethanol and 2 mL DI water. The obtained mixture was then transferred into a 100 mL Teflon-lined stainless-steel autoclave and heated at 80 ºC for 12 h after continuous stirring and ultrasonication for 10 min. The resulting powders were collected via centrifugation, washed thoroughly with ethanol, and vacuum-dried at 60 ºC for 12 h to yield CoS_x-ZnS-n products, where n inherited from the H-ZIF-8@67-n precursors.

To discover the impact of etching in promoting the charge carrier mobility, another series of photocatalysts, i.e., y-CoS_x-ZnS (y = 1, 2, 3, and 4) were prepared by the same sulfidation treatment on the corresponding y-ZIF-8@67-3.5 precursors. That is, CoS_x-ZnS-3.5 and 3-CoS_x-ZnS are literally the same, which will not be emphasized vide infra. For comparison, ZnS cages, ZnS frames, and CoS_x cages were also prepared using the identical sulfidation procedures except for using pure ZIF-8 dodecahedra, H-ZIF-8, and ZIF-67 dodecahedra as the raw materials, respectively.

Characterizations

Powder X-Ray diffraction (XRD) characterizations of the samples were carried out on a Bruker D8 ADVANCR using Cu Kα radiation (40 kV, 40 mA, λ = 0.1543 nm). The BET surface area and porosity of each sample was determined by the N_2 adsorption/desorption isotherms at 77 K

recorded on a Micromeritics ASAP 2020M instrument. Before the N_2 sorption measurements, the sample was degassed at 100 ºC for 12 h. The surface morphologies of the samples were investigated using a field-emission scanning electron microscope (SEM, MERLIN of ZEISS). The morphologies and elemental distributions of the applied samples were observed by transmission electron microscopy (TEM) and high-resolution transmission electron microscopy (HRTEM) using JEOL JEM-2100F with an accelerating voltage of 200 kV. The solid-state diffuse reflectance ultraviolet-visible spectra (UV-vis DRS) were recorded between 200 and 700 nm on a HITACHI U-3010 Spectrophotometer with a $BaSO_4$ plate as a reference. Photoluminescence (PL) emission spectra were measured by using a HITACHI F-7000 spectrophotometer with an excitation wavelength of 310 nm. X-ray photoelectron spectroscopy (XPS) with a Kroatos Axis Ultra DLD system was carried out to determine the electronic states of elements. The metal contents of Zn and Co in the samples were determined quantitatively by atomic absorption spectroscopy (AAS) on a HITACHI Z-2300 instrument. The elemental contents of C, N, and S were measured by an Elementar Vario EL III equipment. $\cdot O_2^-$ and·OH were detected by Electron Paramagnetic Resonance (EPR) on a Bruker EMXnano instrument.

Photoelectrochemical measurements

All the electrochemical measurements were carried out on a CHI 760 E electrochemical system (Shanghai, China), using a typical three-electrode cell, where Pt foil and Ag/AgCl were used as the counter and reference electrode, respectively. The working electrode was prepared as follows: 20 mg of catalyst was dispersed in a mixed solution containing 990 μL ethanol, 990 μL H_2O, and 20 μL 5% Nafion solution by ultrasonication for 10 min. Then, the resulting mixture was dropped on the conductive surface of FTO glass (1 cm^2) and dried at 60 ºC for 12 h. The transient photocurrent was measured under Xe lamp irradiation at a potential bias of 0.65 V in a 0.1 M Na_2SO_4 aqueous solution as the electrolyte, which was filled in a quartz container with a side window. Light off and on was controlled by a baffle. Electrochemical impedance spectroscopy (EIS) measurements were carried out in an aqueous solution containing 5.0 mM $K_3[Fe(CN)_6]$ and 0.1 M KCl as the electrolyte and measured over frequencies ranging from 0.1 Hz to 100 kHz with an amplitude of 5 mV. Mott-Schottky (M-S) plots were measured using the same mode with the frequencies of 1.0, 1.5, and 2.0 kHz.

Photocatalytic hydrogen production

Photocatalytic hydrogen production experiments were carried out in a Pyrex reaction cell, which was connected with a closed gas circulation and evacuation system, as well as a low-temperature circulator to ensure a constant reaction environment (25 °C). A 300 W Xe lamp equipped with AM 1.5 G filter (MICROSOLAR300) was used as the light source to simulate solar energy and provide photons. An online gas chromatograph (GC, TECHCOMP, GC-7900) equipped with a thermal conductivity detector (TCD) and a 5 Å molecular sieve column was used to determine the content of H_2 evolved in the gaseous phase using high-purity argon as the carrier gas. In a typical test, 30 mg photocatalyst was suspended in a 70 mL aqueous solution containing Na_2S (0.75 M) and Na_2SO_3 (1.05 M). The reaction solution was maintained at 25 °C throughout the test. Before irradiation, the suspension was degassed under vacuum for 30 min to completely remove the dissolved oxygen and ensure the anaerobic conditions. For the evaluation of generated H_2, a quantitative gas phase was injected into GC and measured by using an external H_2 standard calibration plot. No H_2 was detected in the comparison test without photocatalyst or light irradiation, implying that H_2 was indeed produced by the photocatalytic process.

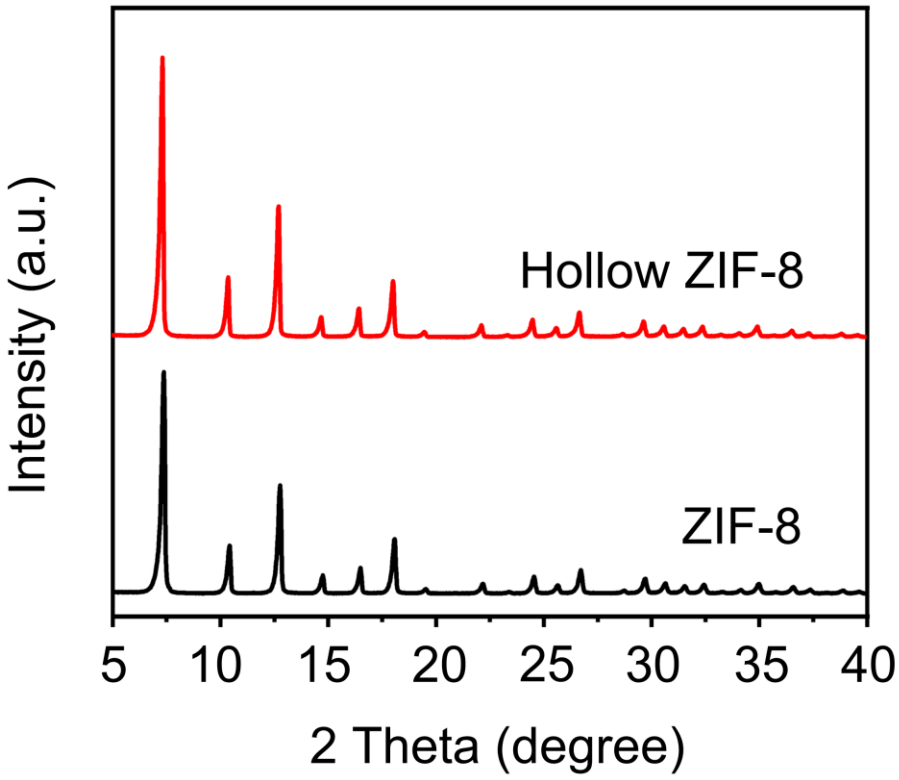

Figure S1. XRD patterns of H-ZIF-8 (red) and ZIF-8 (black).

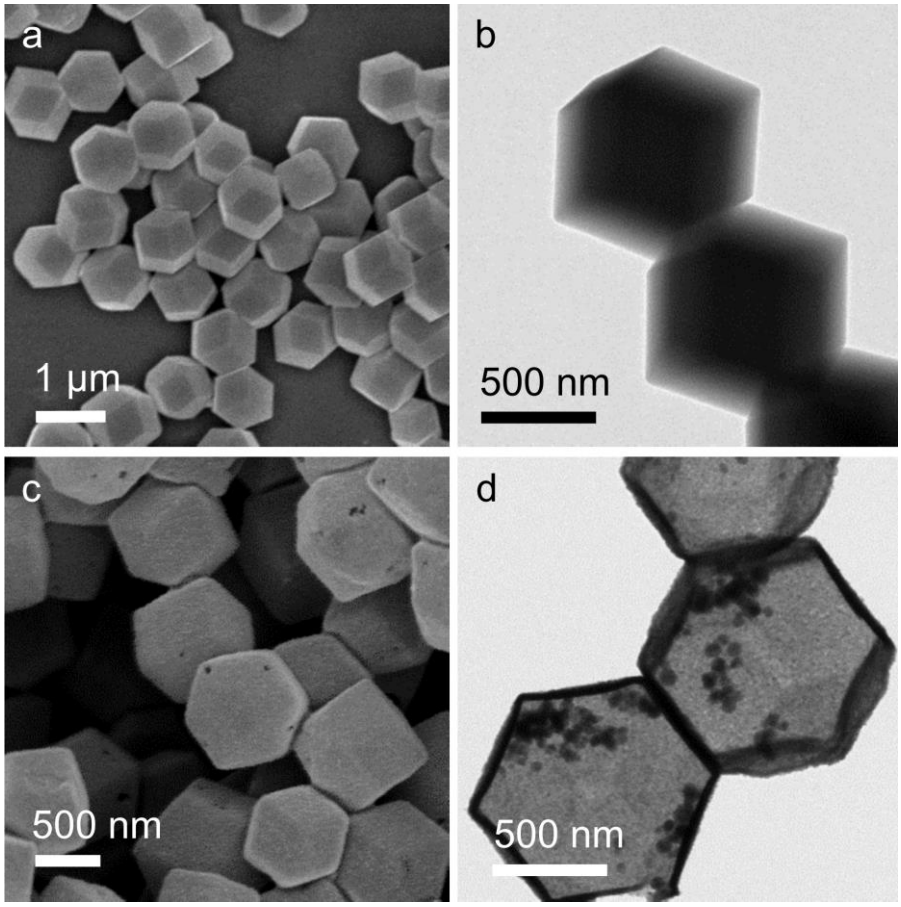

Figure S2. (a) SEM and (b) TEM images of ZIF-8; (c) SEM and (d) TEM images of ZnS derived from ZIF-8 dodecahedron.

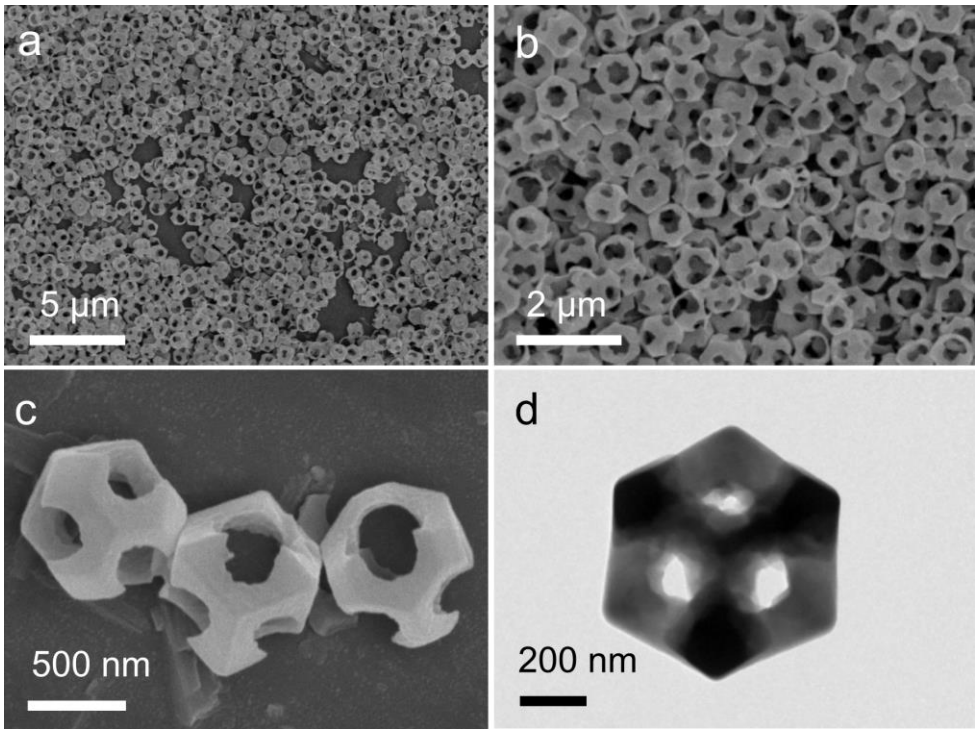

Figure S3. (a-c) SEM images and (d) TEM image of H-ZIF-8 (3-ZIF-8).

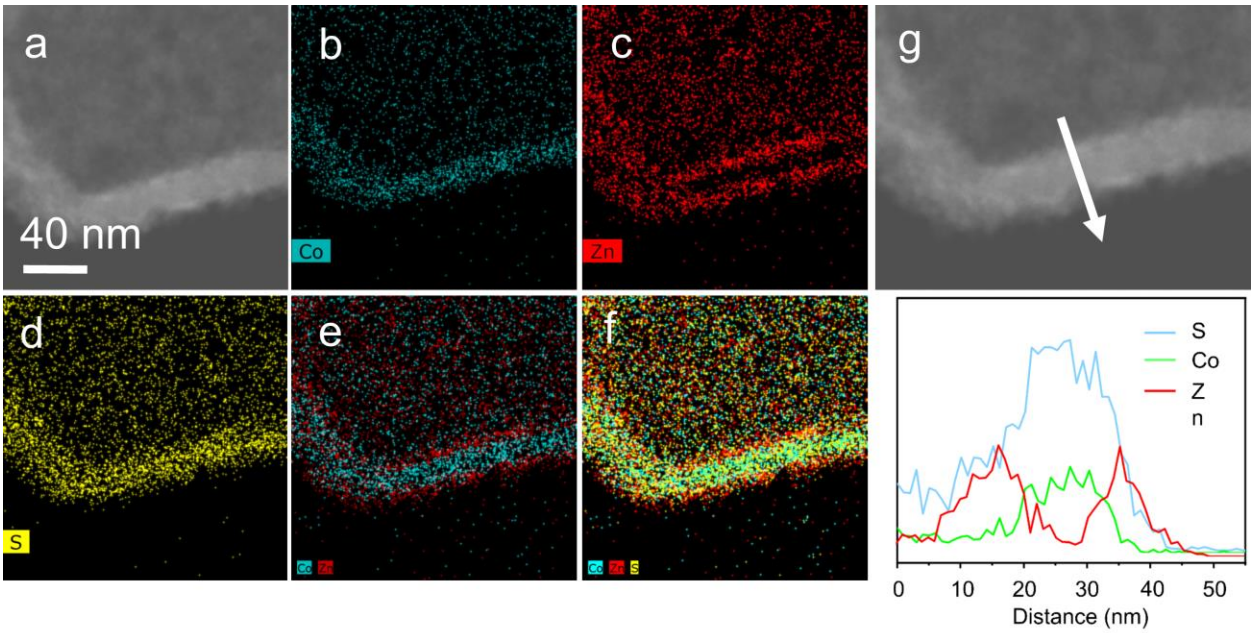

Figure S4. (a) HAADF-STEM, (b-f) EDX mapping and (g) elemental line scan image of the corner of the CoS_x-ZnS nanoframe.

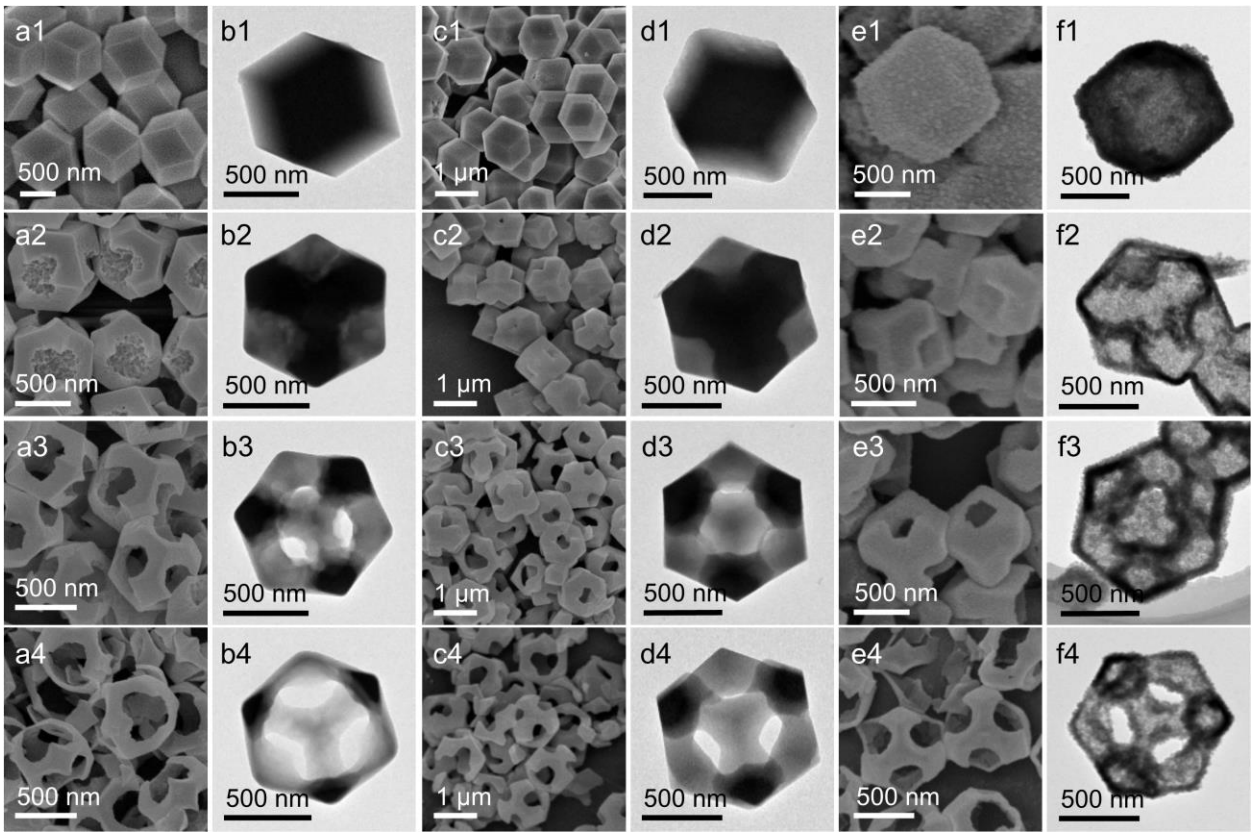

Figure S5. (a1-a4) SEM images and (b1-b4) TEM images of y-ZIF-8 with different etching degrees; (c1-c4) SEM images and (d1-d4) TEM images of y-ZIF-8@67. The Zn/Co molar ratios of y-ZIF-8@67 are all about 3.5; (e1-e4) SEM images and (f1-f4) TEM images of y-CoS_x-ZnS.

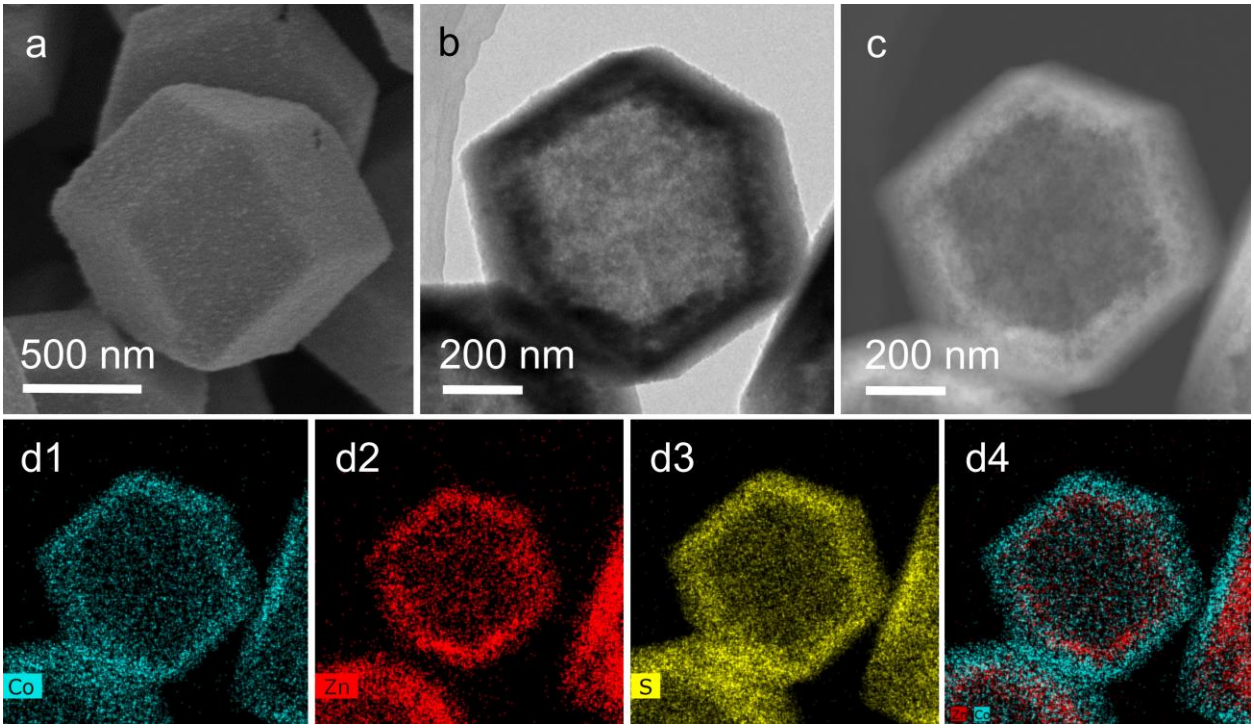

Figure S6. (a) SEM, (b) TEM, (c) HAADF-STEM and (d1-4) EDX mapping images of 1-CoS_x-ZnS.

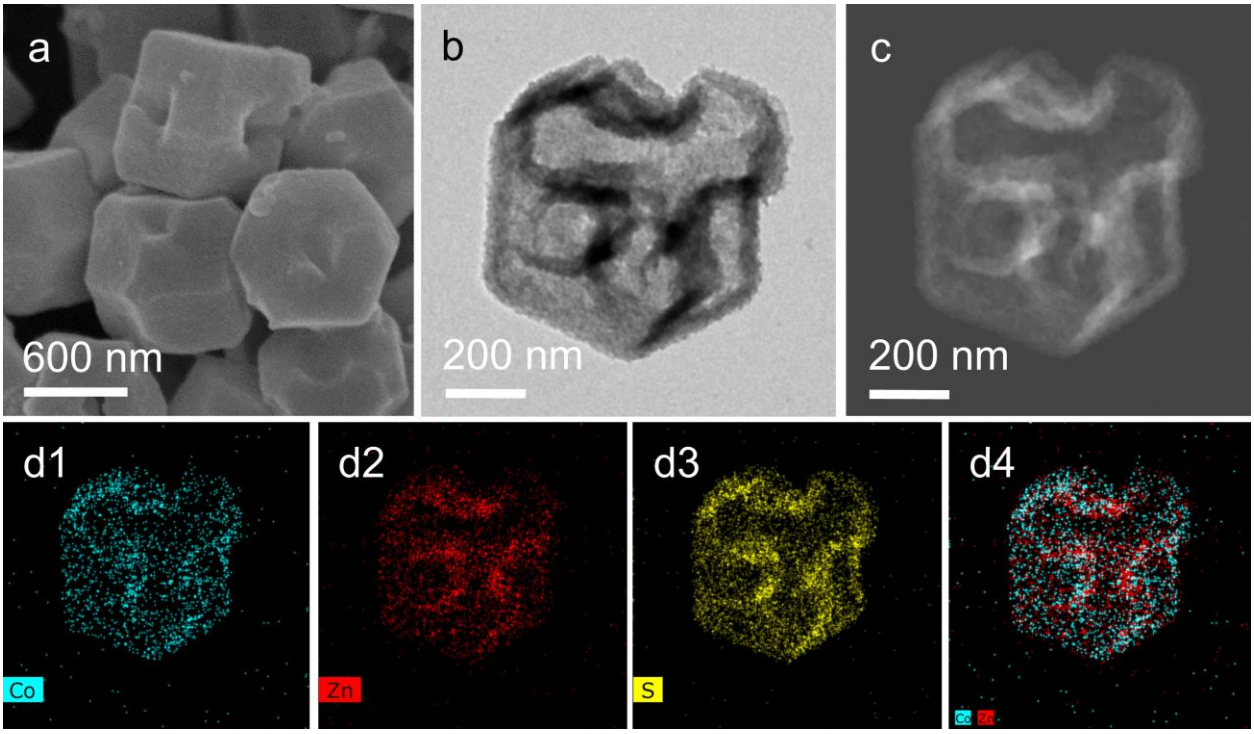

Figure S7. (a) SEM, (b) TEM, (c) HAADF-STEM and (d1-4) EDX mapping images of 2-CoS_x-ZnS.

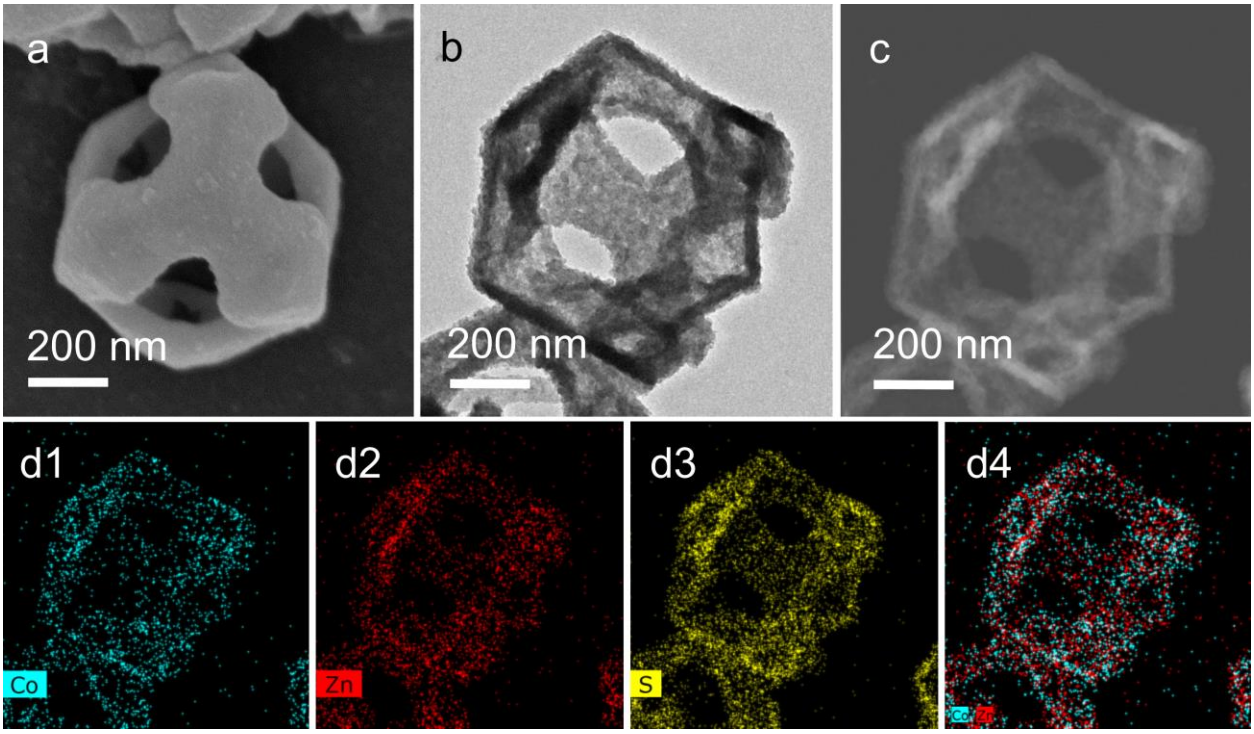

Figure S8. (a) SEM, (b) TEM, (c) HAADF-STEM and (d1-4) EDX mapping images of 4-CoS_x-ZnS.

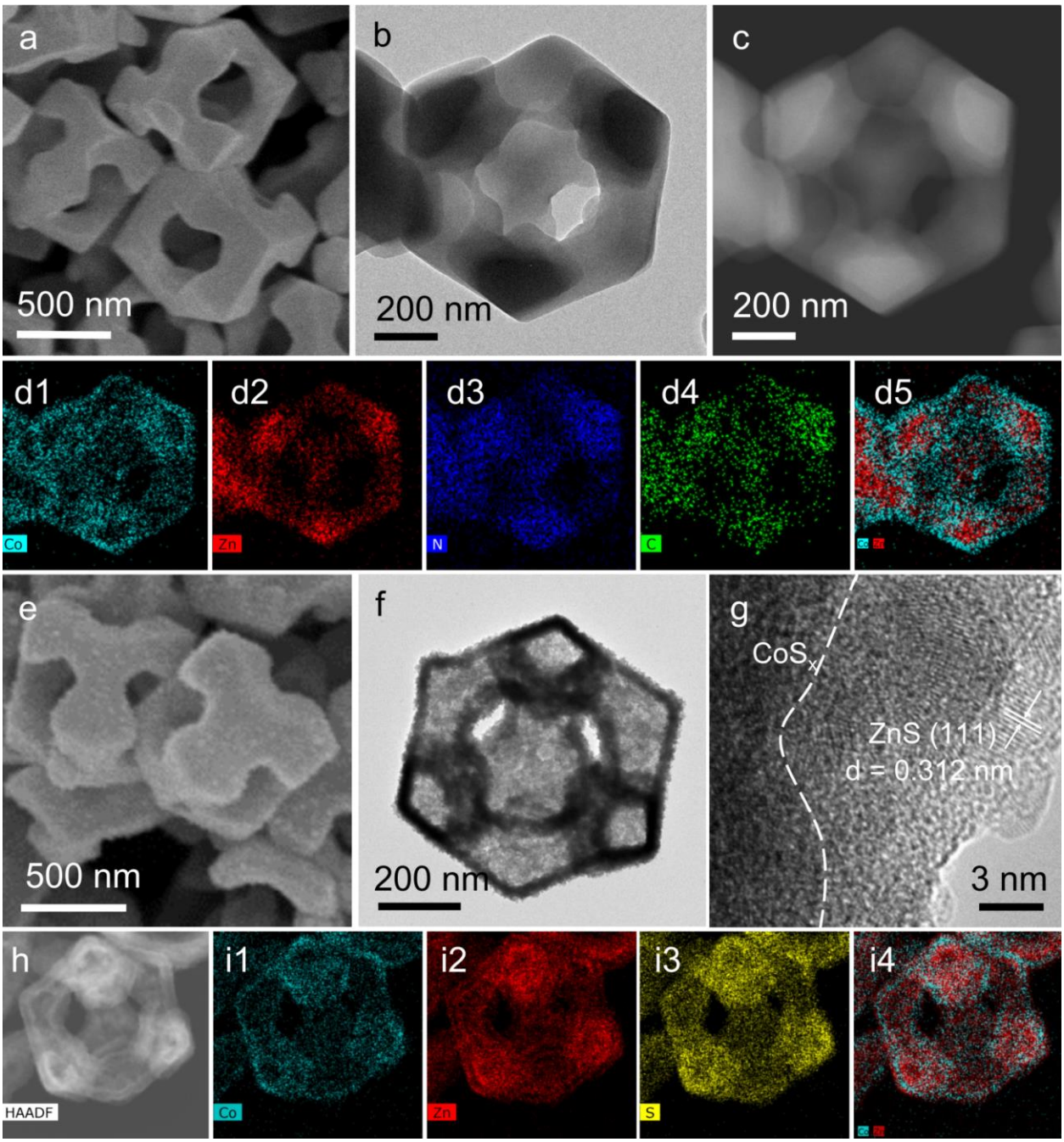

Figure S9. (a) SEM, (b) TEM, (c) HAADF-STEM and (d1-5) EDX mapping images of H-ZIF-8@67-5. (e) SEM, (f) TEM, (g) HRTEM, (h) HAADF-STEM and (i1-4) the EDX mapping images of CoS_x-ZnS-5.

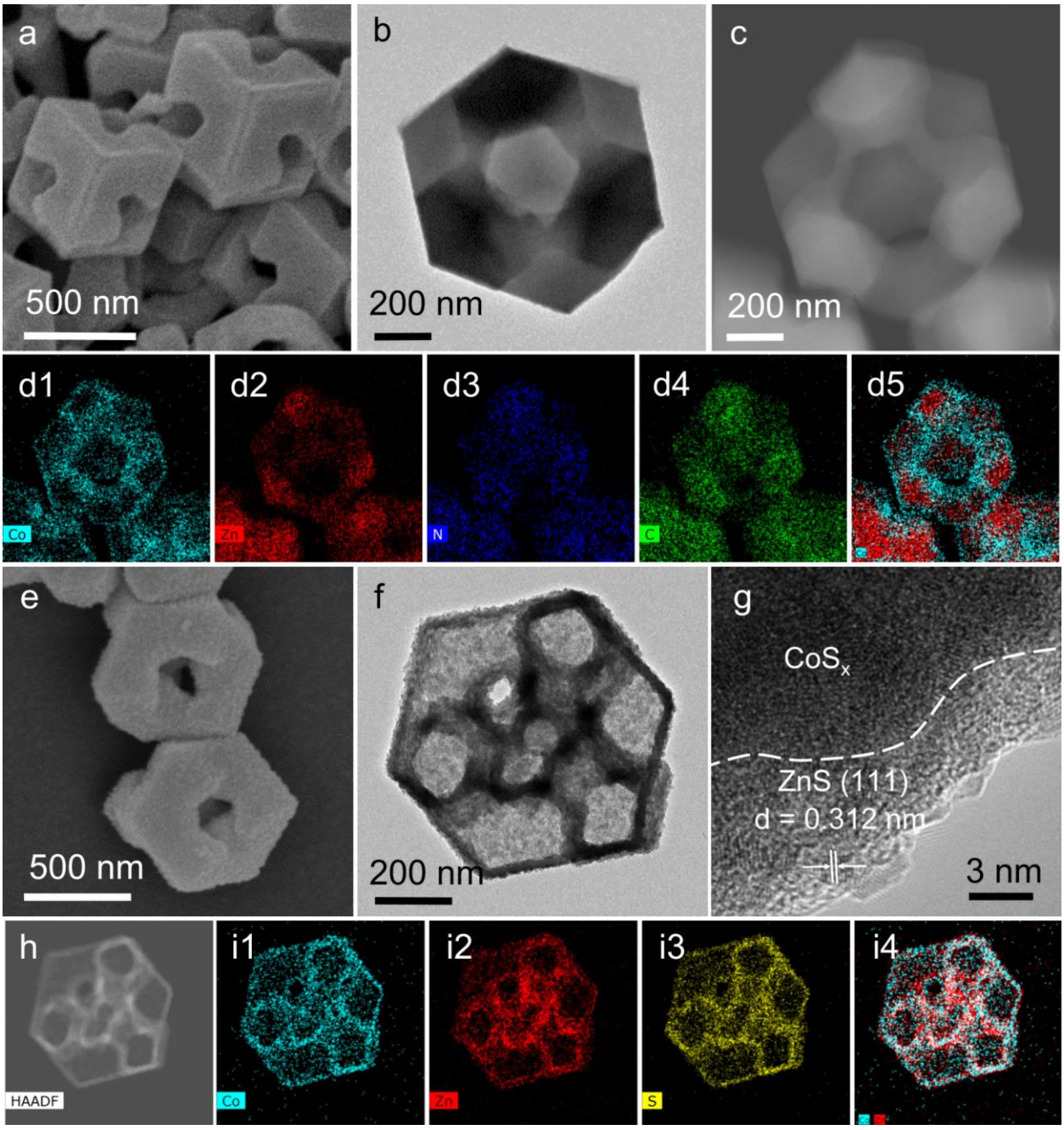

Figure S10. (a) SEM, (b) TEM, (c) HAADF-STEM and (d1-5) EDX mapping images of H-ZIF-8@67-2.5. (e) SEM, (f) TEM, (g) HRTEM, (h) HAADF-STEM and (i1-4) the EDX mapping images of CoS_x-ZnS-2.5.

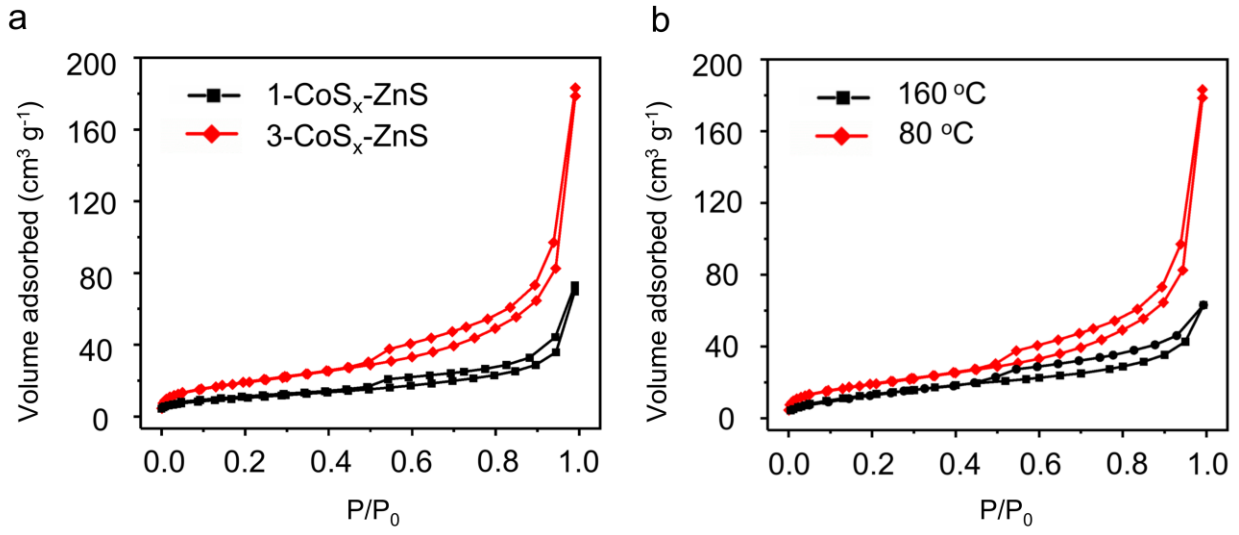

Figure S11. N_2 adsorption/desorption isotherms of (a) S-CoS_x-ZnS-3.5 derived from ZIF-8@67 without etching and normal CoS_x-ZnS-3.5 hollow frames, and (b) CoS_x-ZnS-3.5 hollow frames prepared by the sulfidation process at varied temperatures.

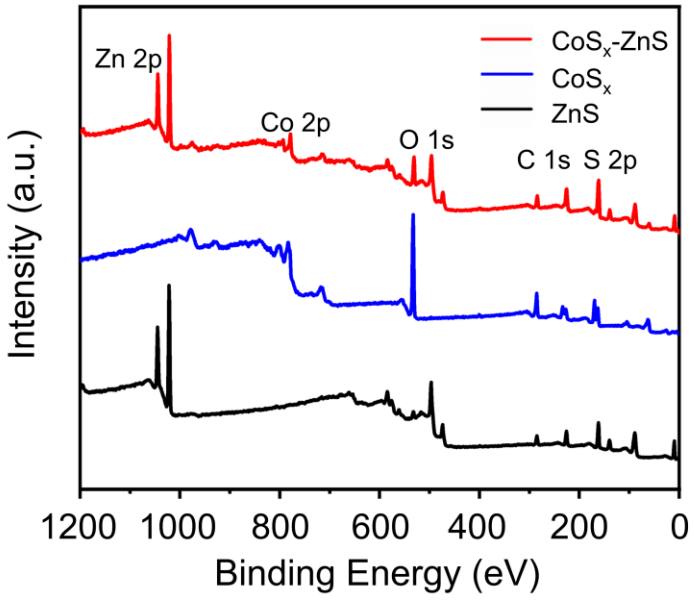

Figure S12. XPS survey spectra of ZnS, CoS_x and CoS_x-ZnS-3.5.

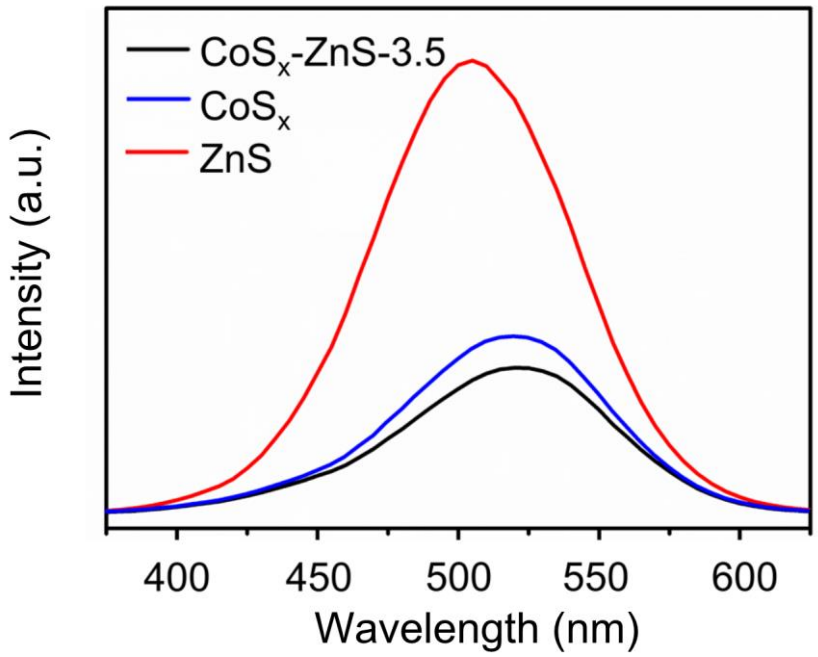

Figure S13. Photoluminescence spectra of ZnS, CoS_x and CoS_x-ZnS-3.5.

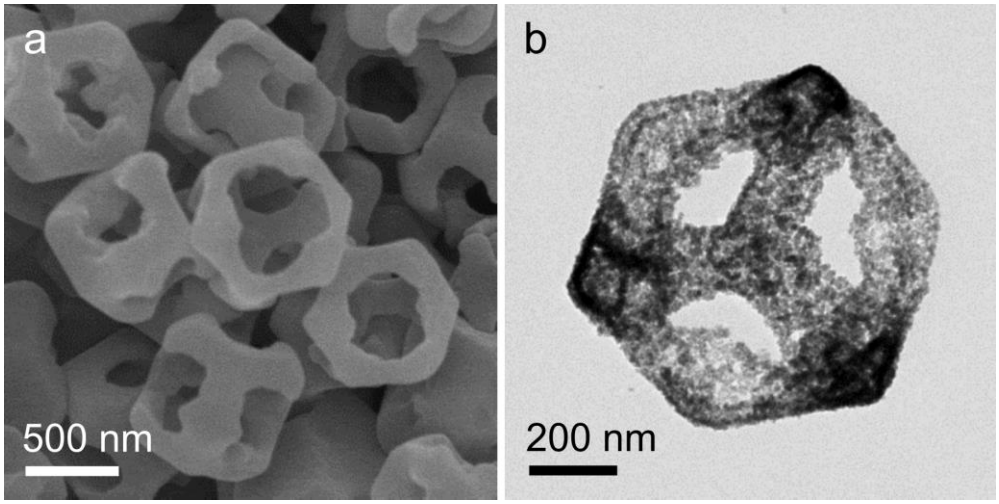

Figure S14. (a) SEM and (b) TEM images of ZnS derived from H-ZIF-8.

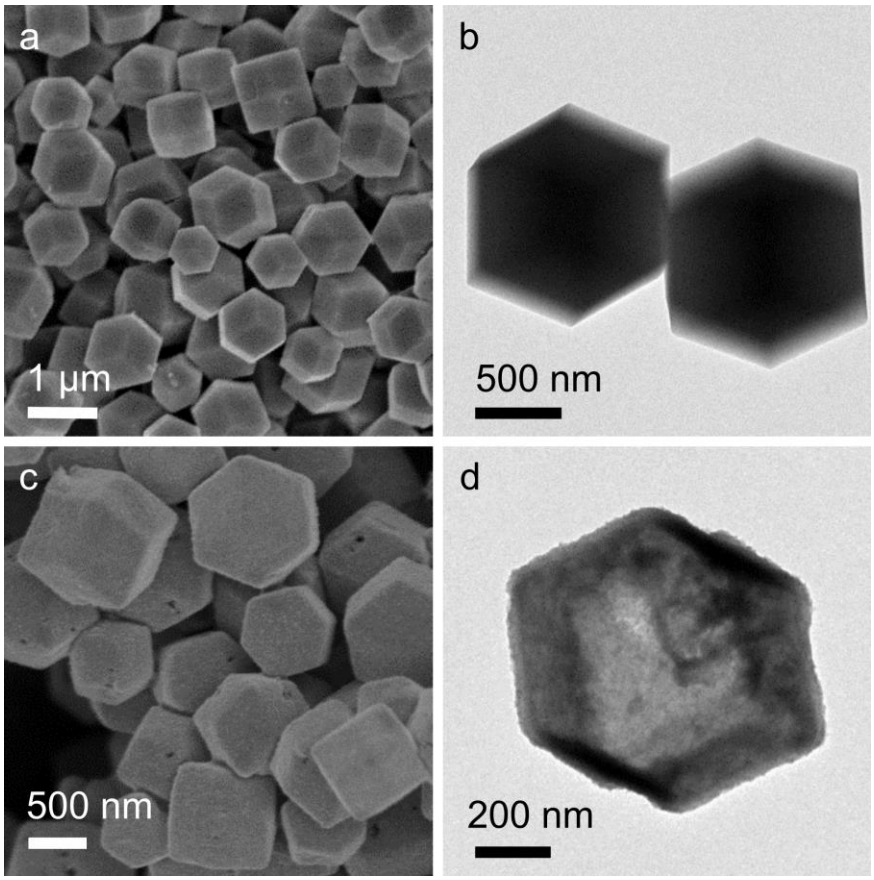

Figure S15. (a) SEM and (b) TEM images of ZIF-67. (c) SEM and (d) TEM images of CoS_x.

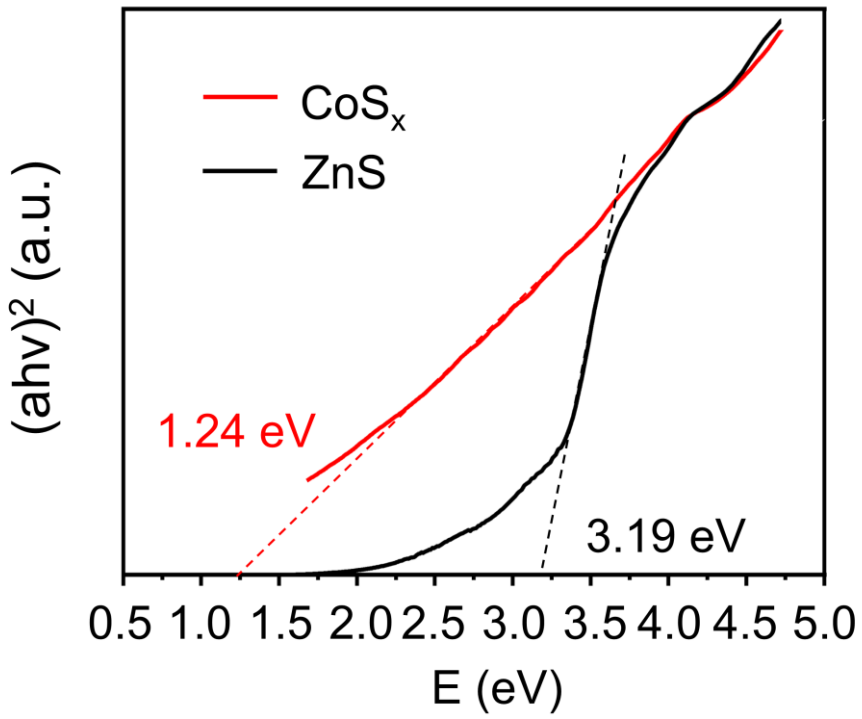

Figure S16. The Plot of $(\alpha hv)^{1/2}$ versus photon energy of the ZnS and CoS_x.

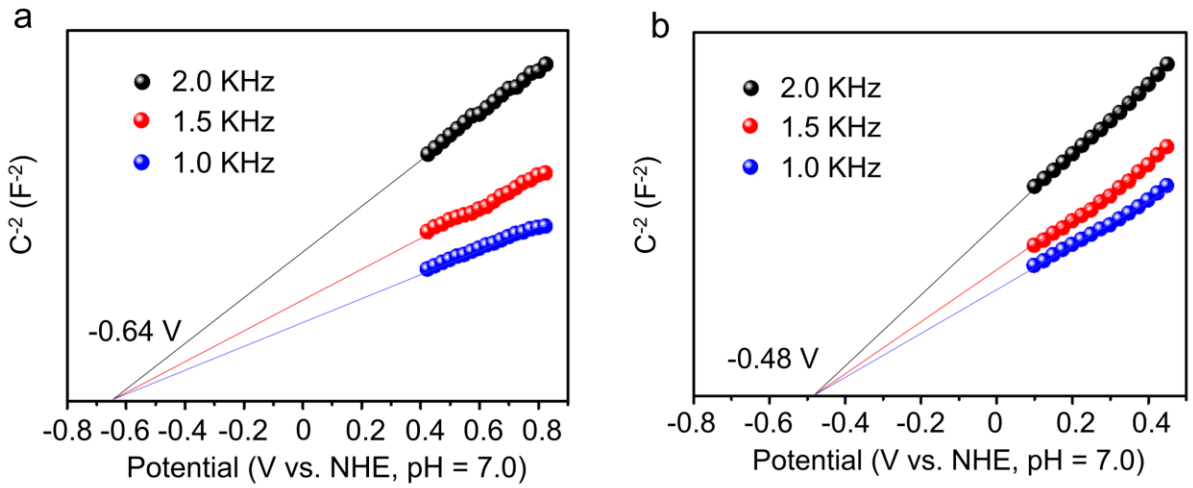

Figure S17. Mott–Schottky plots of (c) ZnS and (d) CoS_x.

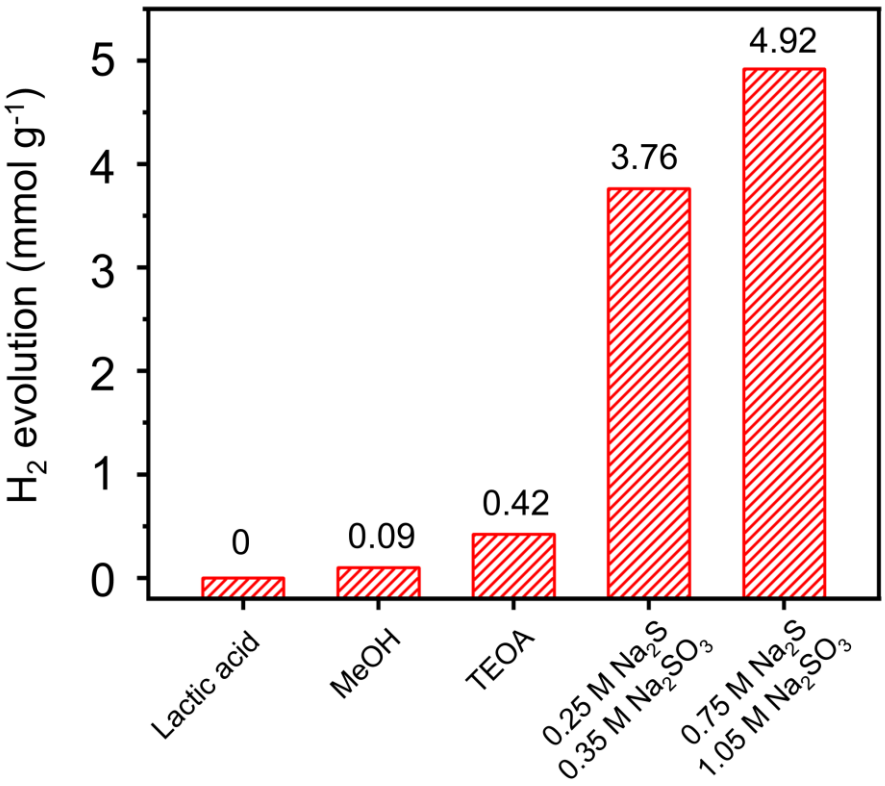

Figure S18. Photocatalytic H_2 evolution on CoS_x-ZnS-3.5 with different sacrificial reagents.

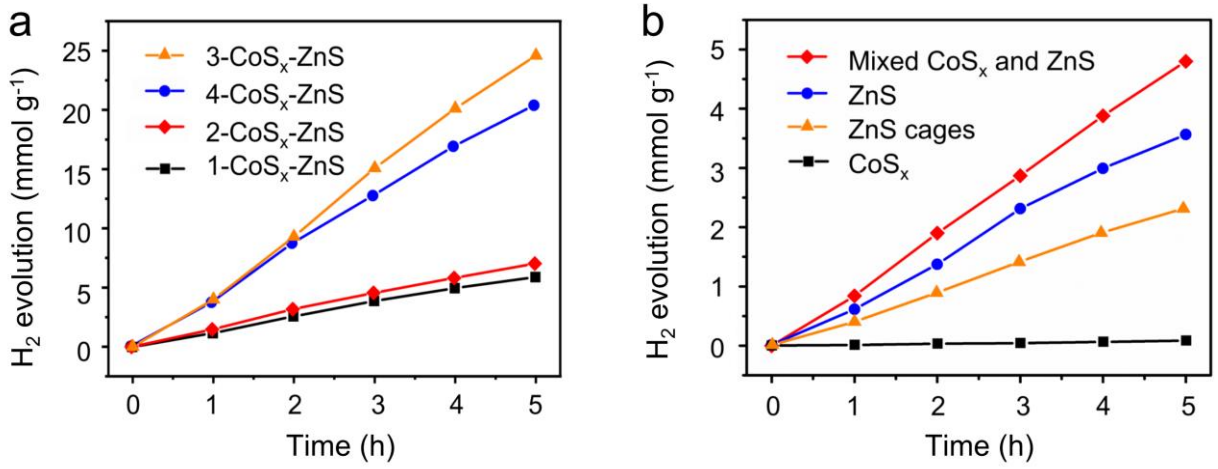

Figure S19. Photocatalytic hydrogen evolution curves of different samples.

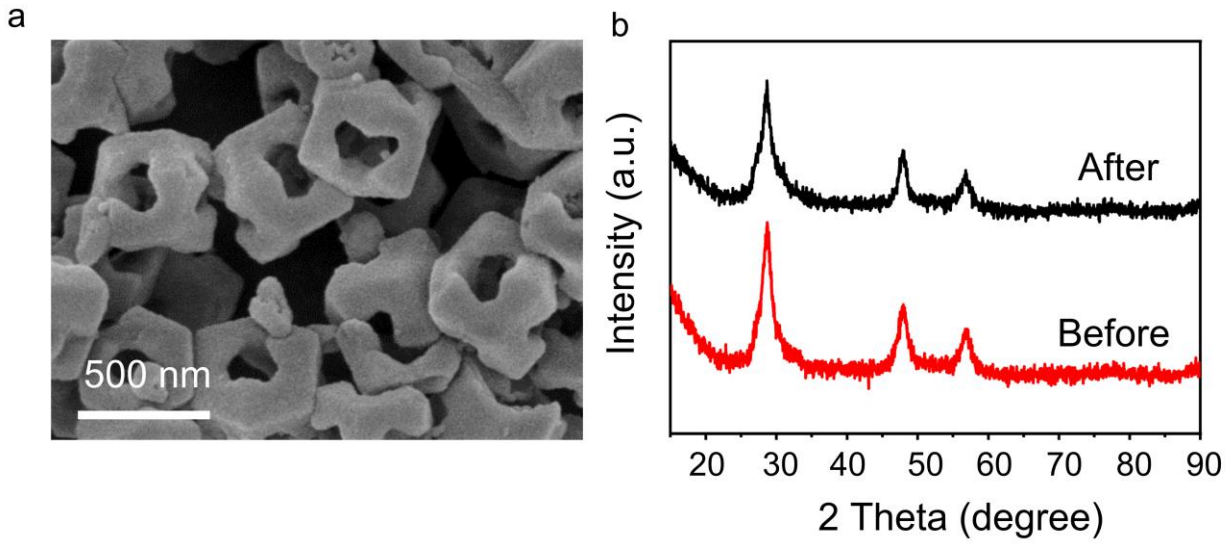

Figure S20. (a) SEM image of CoS_x-ZnS-3.5 after reaction. (b) XRD patterns of CoS_x-ZnS-3.5 before and after recycle test.

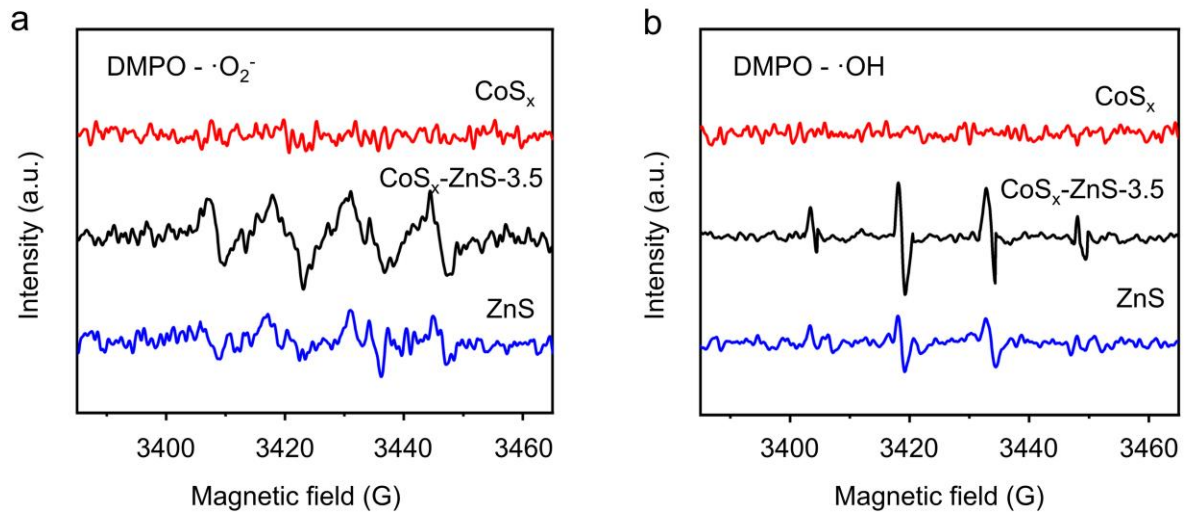

Figure S21. (a) EPR signals of DMPO-·O_2^- in methanol dispersion and (b) EPR signals of DMPO-·OH in aqueous suspension of ZnS, CoS_x and CoS_x-ZnS-3.5. The EPR characterization was performed and the signals were collected after the illumination by Xenon lamp for 3 min.

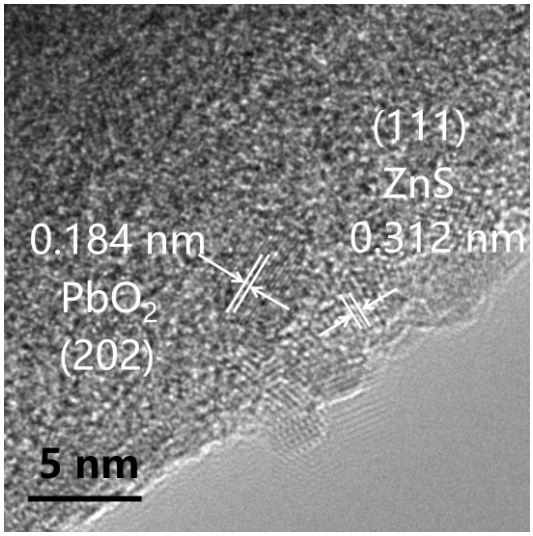

Figure S22. TEM image of CoS_x-ZnS-3.5 photo-deposited with PbO_2 nanoparticles.

Table S1. AAS and element analysis results of different catalysts and the corresponding BET surface areas and pore volumes.

Catalyst	Zn : Co (atomic ratio)[a]	S_{BET} ($m^2\ g^{-1}$)[b]	Pore volume ($cm^3\ g^{-1}$)[c]	Content (wt%)					
				N[d]	C[d]	H	S[d]	Zn[a]	Co[a]
ZnS	-	124	0.23	2.32	6.89	1.68	28.72	58.87	-
CoS_x-ZnS-5	4.95	105	0.22	2.12	7.55	1.53	30.82	48.01	8.75
CoS_x-ZnS-3.5 (3-CoS_x-ZnS)	3.43	90	0.18	1.89	7.95	1.69	31.26	44.05	11.38
CoS_x-ZnS-2.5	2.37	52	0.15	1.81	7.58	1.24	33.25	39.81	15.15
CoS_x	-	16	0.02	1.72	8.24	1.62	35.83	-	50.18
1-CoS_x-ZnS	-	68	0.08	-	-	-	-	-	-
160-CoSx-ZnS-3.5	-	24	0.04	-	-	-	-	-	-

[a] Measured by AAS. [b] BET surface area. [c] Total pore volume. [d] Measured by elemental analysis.

Table S2. Comparison of the H_2-generation rates for various photocatalysts.

Catalyst	Light source	Sacrificial reagent	HER rate ($mmol_{H2}$ h^{-1} g^{-1})	Ref.
CoS_x-ZnS-3.5	**AM 1.5**	**Na_2S-Na_2SO_3**	**4.92**	**This work**
Mixed ZnS/CoS_2	100 mW cm^{-2} Xe arc lamp	Na_2S-Na_2SO_3	0.71	26
ZnS/CoS_2	100 mW cm^{-2} Xe arc lamp	Na_2S-Na_2SO_3	8.0	26
ZnCdS/ZnO/ZnCdS	Visible light	Na_2HPO_4/NaH_2PO_4	2.8	42
ZnS-BP NPs	Visible light	Na_2S-Na_2SO_3	1.56	S1
CoS_2/CdS ZnS-BP NPs	Visible light	Na_2S-Na_2SO_3	1.53	S2
ZnO/ZnS	Visible light	Na_2S-Na_2SO_3	1.35	S3
ZnS/ZnO	Visible light	Na_2S-Na_2SO_3	1.04	S4
CuS/ZnS/CNTF	300 W mercury lamp	Na_2S-Na_2SO_3	0.96	S5
ZnS/g-C_3N_4	Visible light	Na_2S-Na_2SO_3	0.71	29
InP/ZnS	LED light source	H_2A/NaHA	0.69	30
ZnS/Ti_2C_3 MXene	300 W Xe lamp	Na_2S-Na_2SO_3	0.5	S6
ZnS/ZIS-20	AM 1.5	TEOA	0.45	S7
Cu_2ZnSnS_4/ZnS	300 W Xe lamp	Na_2S-Na_2SO_3	0.15	S8

References

1. L. Wang, Y. Hu, F. Qi, L. Ding, J. Wang, X. Zhang, Q. Liu, L. Liu, H. Sun and P. Qu, *ACS Appl. Mater. Inter.*, **2020**, 12, 8157–8167.
2. B. Q. Qiu, C. X. Li, X. Q. Shen, W. L. Wang, H. Ren, Y. Li and J. Tang, *Appl. Catal. A-Gen.*, **2020**, 592, 117377.
3. P. Madhusudan, Y. Wang, B. N. Chandrashekar, W. Wang, J. Wang, J. Miao, R. Shi, Y. Liang, G. Mi and C. Cheng, *Appl. Catal. B-Environ.*, **2019**, 253, 379–390.
4. W. Zeng, Y. Ren, Y. Zheng, A. Pan and T. Zhu, *ChemCatChem*, **2021**, 13, 564–573.
5. C. Chang, Y. Wei and W. Kuo, *Int. J. Hydrogen Energy*, **2019**, 44, 30553.
6. L. Tie, S. Yang, C. Yu, H. Chen, Y. Liu, S. Dong, J. Sun and J. Sun, *J. Colloid Interf. Sci.*, **2019**, 545, 63–70.
7. H. Song, N. Wang, H. Meng, Y. Han, J. Wu, J. Xu, Y. Xu, X. Zhang and T. Sun, *Dalton Trans.*, **2020**, 49, 10816–10823.
8. K. Wang, D. Huang, L. Yu, H. Gu, S. Ikeda and F. Jiang, *J. Colloid Interf. Sci.*, **2019**, 536, 9–16.